Surface & Coatings Technology 204 (2010) 3376–3381

Contents lists available at ScienceDirect

Surface & Coatings Technology

journal homepage: www.elsevier.com/locate/surfcoat

Proposal of new expressions for effects of splat interfaces and defects on effective properties of thermal barrier coatings

Shen Wei, Wang Fu-chi, Fan Qun-bo *, Hua Dan, Ma Zhuang

School of Materials Science and Engineering, Beijing Institute of Technology, Beijing 100081, PR China

ARTICLE INFO

Article history:
Received 21 February 2010
Accepted in revised form 25 March 2010
Available online 9 April 2010

Keywords:
Splat interfaces
Defects
Effective properties
Coatings

ABSTRACT

Based on the law of the conservation of energy, for the first time, novel mathematical formulations are proposed to quantify the influence of splat interfaces and defects on the effective properties of plasma sprayed thermal barrier coatings in spray direction, including the Young's modulus and the thermal conductivity. Combined with finite element solution values and experimental results, a comparison between effect coefficients of splat interfaces and defects shows that splat interfaces account for about 75–80% of the total reduction in the effective Young's modulus, and for about 55–70% of the total reduction in the effective thermal conductivity, indicating that the splat interfaces may have greater influences on the Young's modulus than that on the thermal conductivity.

© 2010 Elsevier B.V. All rights reserved.

1. Introduction

Plasma sprayed thermal barrier coatings (TBCs) have been widely used for the protection of hot-section components in gas turbine. In the current TBCs system, ceramic top-coat provides the thermal insulation and is typically made of Y_2O_3-stabilized ZrO_2 (YSZ), which possesses a suite of desirable properties that make it the material of choice for the top-coat [1]. The splat interfaces and defects (pores and cracks) in ceramic top-coat influence effective properties, including the Young's modulus and the thermal conductivity. To establish quantitative correlations between microstructure and effective properties is needed for optimal design. Relations of microstructures and overall properties of coatings have been studied both theoretically and experimentally [2–5]. Hasselman and Singh [6,7] presented expressions for the effect of microcracks on thermal conductivity and elasticity of brittle ceramics. A model for the microstructure of plasma sprayed coatings involving regions of good and poor contact between lamellae was derived by McPherson [8] to provide an explanation for the much lower thermal conductivity of coatings compared with the bulk material. Ramakrishnan and Arunachalam [9] proposed equations for effective elastic modules of porous solids using the principle of statistical continuum mechanics. Nakamura et al. [10] investigated the effects of pore sizes, shapes, and orientations on the mechanical properties of thermally sprayed ceramic coatings through detailed finite element models with geometries similar to those of actual ceramic containing many embedded pores. Sevostianov and Kachanov [11] estimated the anisotropic properties of plasma sprayed coatings by modeling the dominant elements of porous space (two basic families of pores: parallel and perpendicular). Numerous analytical models and traditional empirical formulas were applied to evaluate effective properties of porous materials [12–19]. Recently, finite element models for actual coating microstructures can be generated by digital image processing, such as object-oriented finite element (OOF) [20] method, which has become one of the most common applications of capturing accurately the effect of real microstructures on effective properties of thermal barrier coatings (TBCs) [21,22]. Nakamura et al. [23] have provided significant information to estimate the effects of splat boundaries through the investigation of thermal cycled coatings based on OOF simulation values and measured values. Up to now, however, the in-depth theoretical research on effects of splat interfaces of TBCs is still rather limited. What's more, no detailed expressions have been proposed to quantify the influence of defects and splat interfaces on the effective properties of plasma sprayed coatings in previous studies.

In the present work, novel mathematical formulations are developed to quantify the contribution of splat interfaces and defects on the effective Young's modulus and the effective thermal conductivity of ZrO_2-8% Y_2O_3 coatings in spray direction. By means of finite element method based on actual microstructural images of YSZ coatings in conjunction with experimental results, a comparison between effects of splat interfaces and defects on the effective properties of plasma sprayed nanostructured YSZ coatings is taken.

2. Expressions for effects of splat interfaces and defects on effective properties

When the stress or the heat flow transfers across the YSZ coating shown in Fig. 1, supposing a unit thickness rectangular plate, the

* Corresponding author. Tel.: +86 10 68911144.
E-mail address: fanqunbo@bit.edu.cn (F. Qun-bo).

0257-8972/$ – see front matter © 2010 Elsevier B.V. All rights reserved.
doi:10.1016/j.surfcoat.2010.03.057

localized effects will be induced by splat interfaces and defects, but will dissipate or smooth out far away from interfaces or defects. Because of the localized effects, nonlinear stress region Ω with volume V_Ω or thermal gradient region Ψ with volume V_Ψ will occur around interfaces and defects, as shown in Fig. 1(a) and (b), respectively.

2.1. Effects of splat interfaces and defects on the effective Young's modulus

If the stress is gradually applied to the coating, all external work will be converted into internal work called strain energy. Suppose the plate is subjected to the uniform stress σ_0 on the top, and the bottom is fixed. If the final displacement is Δh, the external work becomes

$$W = \frac{\sigma_0 \cdot l \cdot \Delta h}{2} \tag{1}$$

where l is the width of the model, while the thickness is unit.

For the coatings without any interior defects, by Hook's law we get

$$U = \int_0^\varepsilon \sigma_0 d\varepsilon \int dx \int dy \int dz = \frac{1}{2}\frac{\sigma_0^2}{E_0}\int_V dV \tag{2}$$

where E_0 is Young's modulus of the bulk material; ε is the strain; V is volume of overall coating. Based on the principle of conservation of energy, $W = U$, the Δh can be expressed as

$$\Delta h = \frac{1}{2}\frac{\sigma_0^2}{E_0}\cdot l \cdot h \cdot \frac{2}{\sigma_0 \cdot l} = \frac{\sigma_0 \cdot h}{E_0} \tag{3}$$

where h is the height of the model.

The effective Young's modulus is obtained according to the following equations:

$$E_{\mathrm{eff}} = \frac{\sigma_0}{\varepsilon_0} = {}^{\sigma_0}/_{\frac{\Delta h}{h}} = E_0 \tag{4}$$

Actually, interfaces and all kinds of defects make ceramic coatings behave inherently very complex. With defects and interfaces inside, Saint-Venant's principle claims that the localized effects caused by any inside defect or interface acting on the body will dissipate or smooth out within regions that are sufficiently removed from the location of defect or interface. Furthermore, the resulting stress distribution at these regions will be the same as that caused by any other statically equivalent load applied to the body without defects inside. Because of the localized effects caused by defects and interfaces, nonlinear stress regions will occur around the defects. Then, the total strain energy is rewritten as

$$U = \frac{1}{2}\frac{\sigma_0^2}{E_0}[(1-\rho)\cdot hl - V_\Omega] + \int_{V_\Omega} \omega dV_\Omega \tag{5}$$

where ρ is the porosity; ω is strain energy density at region Ω and $\int_{V_\Omega}\omega dV_\Omega$ is the strain energy of region Ω.

Considering $W = U$, Δh can be further written as

$$\Delta h = \frac{\frac{\sigma_0^2}{E_0}[(1-\rho)\cdot hl - V_\Omega] + 2\int_{V_\Omega}\omega dV_\Omega}{\sigma_0 \cdot l} \tag{6}$$

The effective Young's modulus can be expressed as

$$E_{\mathrm{eff}} = \frac{\sigma_0}{\varepsilon_0} = {}^{\sigma_0}/_{\frac{\Delta h}{h}} \tag{7}$$

According to Eqs. (6) and (7), the effective Young's modulus can be predicted as

$$\frac{1}{E_{\mathrm{eff}}} = \frac{1}{E_0}\left(1-\rho-\frac{V_\Omega}{hl}\right) + \frac{2\int_{V_\Omega}\omega dV_\Omega}{\sigma_0^2 \cdot hl} \tag{8}$$

here,

$$\frac{2\int_{V_\Omega}\omega dV_\Omega}{\sigma_0^2} = \frac{1}{2E_0}\int_{V_\Omega}\left[\begin{array}{l}\dfrac{\left(\sigma_x^2+\sigma_y^2+\sigma_z^2\right)-2v\left(\sigma_x\sigma_y+\sigma_y\sigma_z+\sigma_z\sigma_x\right)}{\sigma_0^2} \\ +\dfrac{2(1+v)\left(\tau_{xy}^2+\tau_{yz}^2+\tau_{zx}^2\right)}{\sigma_0^2}\end{array}\right]dV_\Omega \tag{9}$$

where σ is the normal stress; τ is the shear stress; and v is the Poisson's ratio. In Eq. (9), the term in square bracket can be reduced as a dimensionless quantity, which is decided by size distributions, orientation direction and morphology of splat interfaces or defects actually.

Considering,

$$\frac{2\int_{V_\Omega}\omega dV_\Omega}{\sigma_0^2} = \frac{f(V_\Omega)}{E_0} \tag{10}$$

Thus,

$$E_{\mathrm{eff}} = E_0 \cdot \frac{hl}{(1-\rho)\cdot hl + [f(V_\Omega) - V_\Omega]} \tag{11}$$

here, V_Ω and $f(V_\Omega)$ are functions related to defects and splat interfaces, independent of the size of models.

If only considering defects, the Young's modulus is written as

$$E_{\mathrm{defects}} = E_0 \cdot \frac{1}{1+\alpha} \tag{12}$$

where $\alpha = [f(V_\Omega(\mathrm{defects}) - V_\Omega(\mathrm{defects})]/hl - \rho$, which is the Young's modulus effect coefficient of defects.

For interfaces only, the Young's modulus is expressed as

$$E_{\mathrm{interfaces}} = E_0 \cdot \frac{1}{1+\beta} \tag{13}$$

where $\beta = [f(V_{\Omega(\mathrm{interfaces})}) - V_{\Omega(\mathrm{interfaces})}]/hl$, which is the Young's modulus effect coefficient of splat interfaces.

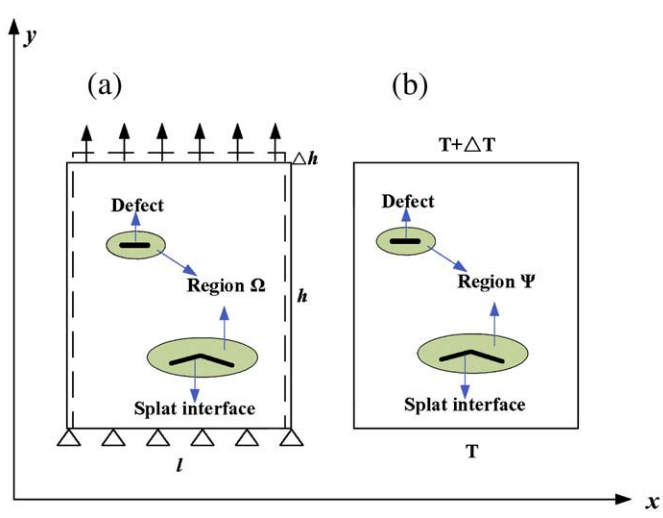

Fig. 1. The YSZ coating plate with defect and splat interface inside. (a) Subject to a uniform normal stress, Ω is the region where nonlinear stress occurs around defects and splat interfaces. (b) Subject to a temperature difference load, Ψ is the region where nonlinear thermal gradient occurs around defects and splat interfaces.

Actually, defects and splat interfaces are affected by each other, V_Ω and $f(V_\Omega)$ will be affected by the locations of defects and splat interfaces additionally. To separate the effects of defects and splat interfaces, the effective Young's modulus is predicted as

$$E_{\text{eff}} = E_0 \cdot \frac{1}{1+\alpha+\beta+\lambda} \tag{14}$$

where λ is the coefficient of interactive effect of defects and splat interfaces. If defects and splat interfaces strengthen the mechanical barrier abilities when interacting with other, the overall effect coefficient of splat interfaces and defects shall be larger than the mathematical sum of splat interfaces and defects effects, namely $\lambda>0$; otherwise, $\lambda<0$.

2.2. Effects of splat interfaces and defects on the effective thermal conductivity

Thermal conductivity K is the property of a material that indicates its ability to conduct heat. It appears primarily in Fourier's law for heat conduction.

$$q = -K\nabla T \tag{15}$$

$$\nabla T = n_0 \frac{\Delta T}{dh} \tag{16}$$

here, q is the heat flux vector, ∇T is the temperature gradient vector, ΔT is the temperature difference, dh is the thickness of conducting surface separating the two temperatures, and n_0 represents vector.

The effective thermal conductivity is determined with the steady-state heat transfer analysis. The top and the bottom of the coating are assigned constant temperature of $T+\Delta T$ and T, and the other two boundaries are kept insulated, shown in Fig. 1(b), such that a temperature difference of ΔT is set up across the plate. Under steady-state conditions, the effective thermal conductivity, K_{eff}, in the heat flow direction can be computed with Fourier's equation:

$$K_{\text{eff}} = \frac{q_\Gamma \cdot h}{\Delta T \cdot l} \tag{17}$$

Here, q_Γ is the total steady-state heat flux per unit thickness through any transverse cross-section of the model.

Meanwhile, the total heat power Q_{sum} in the coating converted by the external work is

$$Q_{\text{sum}} = K_{\text{eff}} \cdot \Delta T \cdot l \tag{18}$$

Considering the localized effects caused by defects or splat interfaces, a nonlinear thermal gradient region Ψ with volume V_Ψ will occur around defects or splat interfaces. Then, the total heat power is written as

$$\begin{aligned} Q_{\text{sum}} &= \int_V K_0 \cdot (\delta\nabla T)^T \nabla T dV \\ &= K_0 \left\{ \frac{\Delta T}{h}[(1-\rho)\cdot hl - V_\Psi] + \int_{V_\Psi} (\delta\nabla T)^T \nabla T dV_\Psi \right\} \end{aligned} \tag{19}$$

where K_0 is the thermal conductivity of the bulk material, and V is the volume of the plate.

According to Eqs. (18) and (19), K_{eff} can be expressed as

$$K_{\text{eff}} = K_0 \left[1-\rho-\frac{V_\Psi}{hl} + \frac{\int_{V_\Psi} (\delta\nabla T)^T \nabla T dV_\Psi}{\Delta T \cdot l} \right] \tag{20}$$

Considering

$$\int_{V_\Psi} \left[\frac{(\delta\nabla T)^T \nabla T}{\frac{\Delta T}{h}} \right] dV_\Psi = f(V_\Psi) \tag{21}$$

where the term in square bracket can be reduced as a dimensionless quantity, which is decided by size distributions, orientation direction and morphology of splat interfaces or defects actually.

Eq. (20) can be rewritten as

$$K_{\text{eff}} = K_0 \left[1-\rho-\frac{V_\Psi}{hl} + \frac{f(V_\Psi)}{hl} \right] \tag{22}$$

here, Ψ and V_Ψ are functions are functions related to defects and splat interfaces, independent of the size of models.

If only considering defects, the thermal conductivity is written as

$$K_{\text{defects}} = K_0(1-\phi) \tag{23}$$

where $\phi = [V_{\Psi(\text{defects})} - f(V_{\Psi(\text{defects})})]/hl + \rho$, which is the thermal conductivity effect coefficient of defects.

For interfaces only, the thermal conductivity is expressed as

$$K_{\text{interfaces}} = K_0(1-\varphi) \tag{24}$$

where $\varphi = [V_{\Psi(\text{interfaces})} - f(V_{\Psi(\text{interfaces})})]/hl$, which is the thermal conductivity effect coefficient of splat interfaces.

Actually, defects and splat interfaces are affected by each other. V_Ψ and $f(V_\psi)$ will be affected by the locations of defects and splat interfaces additionally. To separate the effects of defects and splat interfaces, the effective thermal conductivity is predicted as

$$K_{\text{eff}} = K_0(1-\phi-\varphi-\gamma) \tag{25}$$

where γ is the coefficient of the interactive effect of defects and splat interfaces. If defects and splat interfaces strengthen the heat transfer barrier abilities when interacting with each other, the overall effect coefficient of splat interfaces and defects shall be larger than the sum of splat interfaces and defects effects ,namely $\gamma>0$; otherwise, $\gamma<0$.

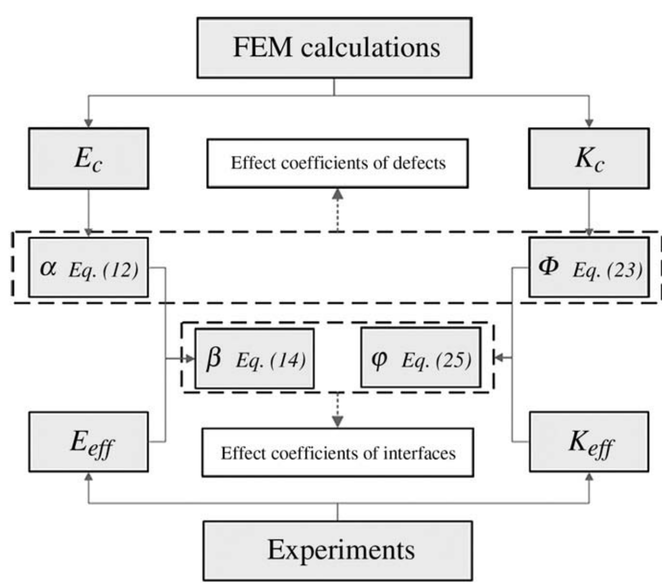

Fig. 2. Flowchart illustrating the methodology for predicting effect coefficients.

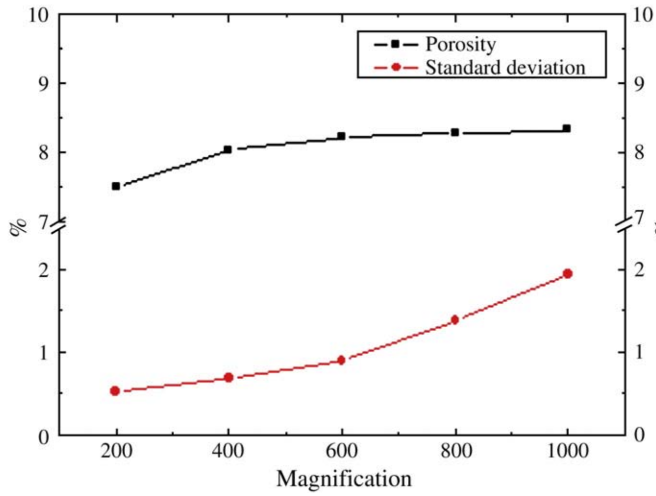

Fig. 3. Porosity and standard deviation as function of magnification for plasma sprayed YSZ coating. SEM images at ×600 are chosen for higher porosity and lower standard deviation.

3. Comparisons between effect coefficients of splat interfaces and defects

As shown in Fig. 2, instead of calculating the effective properties directly using the equations mentioned above, we predict the thermal conductivity and the Young's modulus of coatings by finite element method (FEM) at first. To capture the real characteristics of the microstructures, digital image processing technique is employed [24]. Two important issues should be considered. Firstly, the model sample must be large enough to contain sufficient microstructural features. Secondly, detailed microstructural features must be included in the model to reflect the real microstructure of coatings [23]. As seen in Fig. 3, the porosity is slightly increasing with increasing picture magnification from ×200 to ×1000, while the standard deviation is increasing rapidly. In our simulation, scanning electron microscopy (SEM) images at ×600 with an average porosity of 8.28% is used. In this paper, over 200 images are selected and more than 70,000 quadrangle elements are used in each finite element mesh, as shown in Fig. 4(a) and (b). Since the Young's modulus and the thermal conductivity of air are very small as compared to that of the bulk material, zero Young's modulus and zero thermal conductivity are assumed within defect areas. While the Young's modulus and thermal conductivity of fully dense bulk material are chosen as $E_0 = 200$ GPa and $K_0 = 2.3$ W/mK, respectively. Incidentally, those extremely thin microcracks and micropores, which are not shown in these images due to the limited resolution of micrograph, are not considered in our simulation for their ignorable influences on the effective properties (see more discussion in Ref. [23]).

With the aid of ANSYS code in conjunction with the Fourier's equation and the stress equation (see more details in Refs. [21,23]), the apparent Young's modulus and the apparent thermal conductivity, namely E_c and K_c, are computed in Table 1. It might be noted that

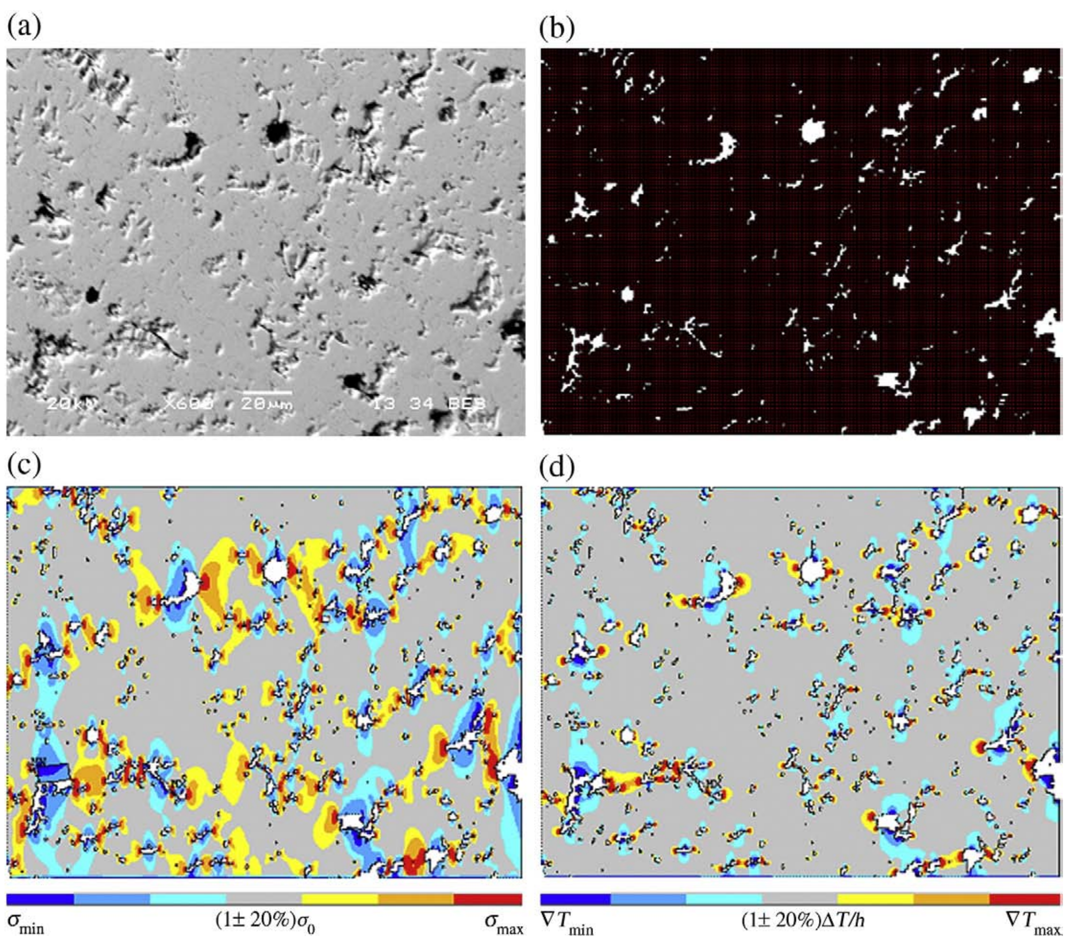

Fig. 4. Finite element model and distributions of stress and thermal gradient. (a) A SEM cross-section image of YSZ coating (212 μm × 159 μm). (b) Finite element model according with SEM image. (c) Stress profile. Grey color represents normal region ($1 \pm 20\%\ \sigma_0$) not affected by defects, while other colors indicate nonlinear stress region Ω. (d) Thermal gradient profile. Grey color represents normal region ($1 \pm 20\%\Delta T/h$) not affected by defects, while other colors indicate nonlinear thermal gradient region Ψ.

Table 1
Estimated effective properties and effect coefficients of YSZ coatings.

	E_X	E_Y	K_X	K_Y
Computed values	142 GPa	132 GPa	1.85 W/mK	1.78 W/mK
Experimental results		56 GPa		1.08 W/mK
Effect coefficients		$\alpha=0.515$		$\phi=0.226$
		$\beta=2.056-\lambda$		$\varphi=0.304-\gamma$

the effects of splat interfaces can not be taken into account by FEM, because the interface properties are unknown and not introduced. The difference between FEM solution results and values of bulk material can be attributed to defects (pores and cracks). Fig. 4 shows distributions of stress in spray direction and thermal gradient under steady-state conditions, grey color represents normal regions ($1\pm 20\%\ \sigma_0$ or $1\pm 20\%\ \Delta T/h$) not affected by defects, while other colors indicate nonlinear stress region and thermal gradient region. In Fig. 4 (c) and (d), the stress contours and thermal gradient contours clearly illustrate the effects of defects. There are obvious concentrations of stress and thermal gradient around defects. Generally, higher stresses or thermal gradients contribute to lower effective Young's modulus or thermal conductivity. The Young's modulus and the thermal conductivity of the coating in the spray direction namely E_e and K_e are measured as 56 GPa and 1.08 W/mK, respectively. As shown in Fig. 2, the difference between calculated FEM results and experimental values is attributed to splat interfaces and interactive effects of defects and splat interfaces. The effect coefficient can be further expressed as

$$\begin{cases} 132 = 200\dfrac{1}{1+\alpha} \\ 56 = 200\dfrac{1}{1+\alpha+\beta+\lambda} \end{cases} \tag{26}$$

$$\begin{cases} 1.78 = 2.3(1-\phi) \\ 1.24 = 2.3(1-\phi-\varphi-\gamma) \end{cases} \tag{27}$$

Thus,

$$\begin{cases} \alpha = 0.515 \\ \beta = 2.056-\lambda \end{cases} \tag{28}$$

$$\begin{cases} \phi = 0.226 \\ \varphi = 0.304-\gamma \end{cases} \tag{29}$$

To compare effect coefficients of defects and splat interfaces, additional methods are required to estimate λ and γ. Three artificial finite element models with dimensions 25 μm × 25 μm and more than 20,000 elements are designed in Fig. 5: all of the defects are idealized and assumed to be spheroid elements with the aspect ratios of $b/a = 0.6$ (a and b are major and minor axes, $a = 0.7$ μm) in Fig. 5(a); all of the interfaces are idealized and assumed to be rectangle elements with the size of 3.25 μm × 0.125 μm in Fig. 5(b); Fig. 5(c) shows the model containing defects and interfaces together. Corresponding effective properties and effect coefficients are shown in Table 2. E_Y and K_Y of the model in Fig. 5(a), only representing the defects inside of coating, are approximately equal to computed values in Table 1. And K_Y and E_Y of the model in Fig. 5(c), representing the defects and interfaces inside of coating, are close to the experimental results. Hence, β and φ of the model in Fig.5(b) could indicate the effect coefficients of splat interfaces. By certain values of α, β and ϕ, φ, λ and γ are calculated as 0.279 and −0.178, respectively. To ensure the methodology's stability and reduce its sensitivity, more models, whose E_Y and K_Y are similar to the ones' in Table 1, are chosen to further make sure the range of γ and λ. Ultimately, we get

$$\begin{cases} 0<\gamma<\alpha \\ -\phi<\lambda<0 \end{cases} \tag{30}$$

Thus, β and φ can be further predicted as

$$\begin{cases} 3\alpha<\beta<4\alpha \\ 1.35\phi<\varphi<2.35\phi \end{cases} \tag{31}$$

A comparison between effect coefficients of defects and splat interfaces, namely α and β, shows that the Young's modulus effect coefficient of splat interfaces is more than triplicate effect coefficients of defects, indicating that splat interfaces have much greater influences on the Young's modulus than defects. Comparing ϕ and φ it can be found that the splat interfaces makes more contribution than defects in defining the thermal conductivity of plasma sprayed coatings.

It is found that splat interfaces play major important role in defining effective properties. Actually, it appears that splat interfaces account for about 75–80% ($75\%<\frac{\beta}{\alpha+\beta}<80\%$) of the total reduction in the effective Young's modulus, and for about 55–70% ($55\%<\frac{\varphi}{\phi+\varphi}<70\%$) of the total reduction in the effective thermal conductivity, indicating that the splat interfaces have greater influences on the Young's modulus than that on the thermal conductivity; their role as barriers to mechanical force

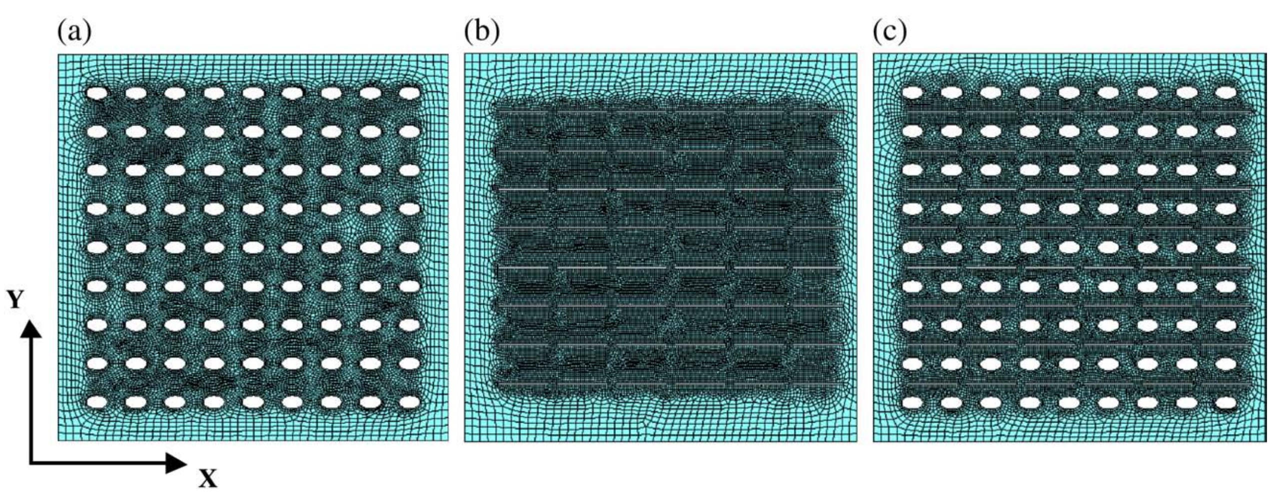

Fig. 5. Finite element models used to estimate effective properties and effect coefficients. (a) Idealized spheroid elements representing the defects in coatings. (b) Rectangle elements representing the splat interfaces in coatings. (c) The model containing defects and interfaces together.

Table 2
Computed effective properties and effect coefficients of artificial models.

	E_Y (GPa)	α, β, γ	K_Y (W/mK)	ϕ, φ, λ
Fig. 5(a)	131	$\alpha = 0.527$	1.74	$\phi = 0.243$
Fig. 5(b)	74	$\beta = 1.703$	1.15	$\varphi = 0.500$
Fig. 5(c)	57	$\gamma = 0.279$	1.00	$\lambda = -0.178$

transfer is more significant than that as barriers to physical thermal transfer. In future work, additional methods are required to verify the underlying nature of splat interfaces role in plasma sprayed TBCs.

4. Conclusions

(1) Based on the law of the conservation of energy, novel expressions are proposed to quantify the influence of splat interfaces and defects on the effective Young's modulus and thermal conductivity of plasma sprayed thermal barrier coatings.
(2) Finite element models according to realistic microstructure of coatings are generated to compute the apparent Young's modulus and the apparent thermal conductivity. Meanwhile, effect coefficients of defects are calculated by means of analytical equations.
(3) Combining with finite element solution values and experimental results, effect coefficients of splat interfaces are evaluated. A comparison between effect coefficients of splat interfaces and defects shows that splat interfaces account for about 75–80% of the total reduction in the effective Young's modulus, and for about 55–70% of the total reduction in the effective thermal conductivity, which indicates that the splat interfaces have greater influences on the Young's modulus than that on the thermal conductivity.

Acknowledgements

We acknowledge the funding supports of the project (No. 50801005) from the Chinese National Natural Science Foundation.

References

[1] N.P. Padture, M. Gell, E.H. Jordan, Science 296 (2002) 280.
[2] R. McPherson, P. Cheang, High Perform. Ceram. Films Coat. 27–30 (1991) 277.
[3] S. Gu, T.J. Lu, D.D. Hass, H.N. Wadley, Acta Mater. 49 (2001) 2539.
[4] J.R. Nicholls, K.J. Lawson, A. Johnstone, D.S. Rickerby, Surf. Coat. Technol. 151–152 (2002) 383.
[5] J.S. Wallace, J. Ilavsky, J. Therm. Spray Technol. 7 (1998) 521.
[6] D.P.H. Hasselman, J. Compos. Mater. 12 (1978) 403.
[7] D.P.H. Hasselma, J.P. Singh, Am. Ceram. Soc. Bull. 58 (1979) 856.
[8] R. McPherson, Thin Solid Films. 112 (1984) 89.
[9] N. Ramakrishnan, V.S. Arunachalam, J. Mater. Sci. 25 (1990) 3930.
[10] T. Nakamura, G. Qian, C.C. Berndt, J. Am. Ceram. Soc. 83 (2000) 578.
[11] I. Sevostianov, M. Kachanov, Acta Mater. 48 (2000) 1361.
[12] M. Kachanov, Int. J. Solids Struct. 23 (1987) 23.
[13] Y.H. Zhao, G.P. Tandom, G.J. Weng, N. Brunswich, N. Jersey, Acta Mech. 76 (1989) 105.
[14] K.A. Khor, Y.W. Gu, Thin Solid Films 372 (2000) 104.
[15] D.D. Hass, A.J. Slifka, H.N. Wadley, Acta Mater. 49 (2001) 973.
[16] J. Wu, X. Wei, N.P. Padture, P.G. Klemens, M. Gell, P. Eugenio García, M.I. Miranzo, J. Osendi, Am. Ceram. Soc. 85 (2002) 3031.
[17] J.W. Ju, T.M. Chen, Acta Mech. 103 (1994) 123.
[18] J. Argyris, I. St. Doltsinis, M. Eggers, R. Handel, Comput. Methods Appl. Mech. Eng. 111 (1994) 203.
[19] M. Kachanov, I. Tsukrov, B. Shafiro, Appl. Mech. Rev. 47 (1994) 151.
[20] S.A. Langer, W.C. Carter, E.R. Fuller Jr., Object Oriented Finite Element Analysis for Materials Science, Center for Theoretical and computational Materials Science and the Information Lab. at the NIST, 1997, URL: www.ctcms.nist.gov/oof/.
[21] P. Michlik, C. Berndt, Surf. Coat. Technol. 201 (2006) 2369.
[22] A.D. Jadhav, N.P. Padture, E.H. Jordan, M. Gell, P. Miranzo, J.E. Fuller, Acta Mater. 54 (2006) 3343.
[23] Z. Wang, A. Kulkarni, S. Deshpande, T. Nakamura, H. Herman, Acta Mater. 51 (2003) 5319.
[24] S. Wei, F. Qun-bo, W. Fu-chi, M. Zhuang, Comput. Mater. Sci. 49 (2009) 600.